Supporting Information to:

'Organic Matter Influences Transformation Products of Ferrihydrite Exposed to Sulfide'

Laurel K. ThomasArrigo,*[a] Sylvain Bouchet,[a] Ralf Kaegi,[b] and Ruben Kretzschmar[a]

[a]*Soil Chemistry Group, Institute of Biogeochemistry and Pollutant Dynamics, Department of Environmental Systems Science, ETH Zurich, Universitätstrasse 16, CHN, CH-8092 Zurich, Switzerland*

[b]*Eawag, Swiss Federal Institute of Aquatic Science and Technology, Überlandstr. 133, CH-8600 Dübendorf, Switzerland*

(20 Pages, 10 Figures, 9 Tables)

Table of contents

*Corresponding author: laurel.thomas@usys.ethz.ch

1. Structure and elemental composition of organic ligands

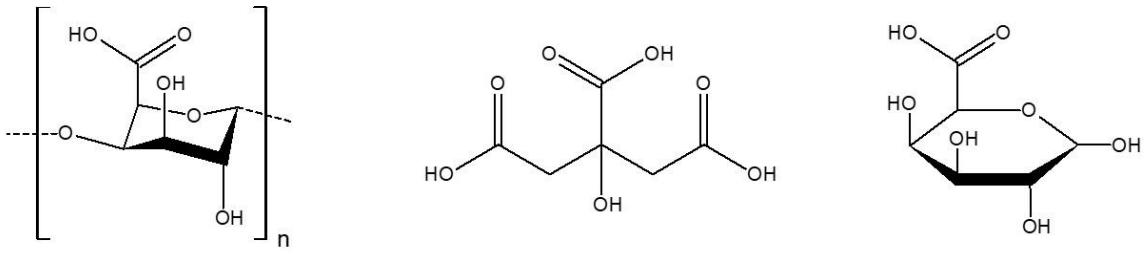

Figure S1. Chemical structures of the model organic ligands used in this study. pK_a(polygalacturonic acid) = 3.48, $pK_{a1,2,3}$(citric acid) = 3.13, 4.76, 6.4, pK_a(galacturonic acid) = 3.48 (25°C).

Table S1. Elemental composition (including impurities) of organic ligands used in coprecipitate synthesis.[a]

Organic ligand	Short name	M_w	C	Al	Ca	Cl	Fe	K	Mg	Na	P	S	Si
		Da	mg/g	µg/g									
Polygalacturonic acid	PGA	25-50×10^3	373	20	44	-[b]	14	45	13	1873	33	-	617
Citric acid	CA	192	350	34	-	-	84	-	77	1789	52	-	433
Galacturonic acid	GA	194	329	17	34	38	10	91	69	106100	78	211	600

[a]Determined by X-ray flurescence (XEPOS, Spectro) and an elemental analyzer (C, CHNS-932, LECO, *n*=2).
[b]Elemental concentrations of <20 ug/g were not included in the table or are indicated with a dash (-).

2. Coprecipitate synthesis and characterization

All solutions used for the synthesis of (co)precipitates were prepared from doubly deionized (DDI) water (Milli-Q®, Millipore, 18.2 MΩ·cm). The synthesis of 2-line ferrihydrite (Fh) followed standard methods;[1] the pH of a solution containing 100 mmols of Fe(III) as $Fe(NO_3)_3 \cdot 9H_2O$ (Merck) was raised to pH 7.0±0.1 by the rapid addition of 1 M NaOH (Titrisol®) under vigorous stirring (1200/min). To obtain the ferrihydrite-OM coprecipitates with similar C/Fe molar ratios, between 150-250 mg of PGA (≥90% (enzym.), Sigma-Aldrich), CA (≥98%, Sigma-Aldrich), or GA (≥98%, Sigma-Aldrich) was equilibrated overnight in darkness in 1 L DDI water adjusted to pH 7.0 with 1 M NaOH under vigorous stirring (1200/min). The ligand-containing solutions were then acidified to pH 4.0 with 1 M HNO_3 (Titrisol®) and purged with N_2(g) for 15 min. Then, 50 mL of a solution containing 10 mmols of Fe(III) as $Fe(NO_3)_3 \cdot 9H_2O$ (Merck) were added, followed by the addition of 1 M NaOH as described in the synthesis of ferrihydrite. Resulting (co)precipitates were repeatedly centrifuged at 3500*g* for 15 min, decanted, and resuspended in 700 mL DDI water until the electrical conductivity of the supernatants was ≤100 µS/cm. The suspensions were then shock-frozen by dropwise injection into liquid N_2,[2] freeze-dried, manually

homogenized with a mortar and pestle, and stored in brown glass in a desiccator until use. The synthetic ferrihydrite-OM coprecipitates are hereafter named Fh-PGA, Fh-CA, and Fh-GA.[3]

Unreacted coprecipitates were additionally imaged with electron microscopy (EM), shown in Figure S3. For these analyses, ~2 mg of solid-phase material was re-suspended in 10 µL of DDI water and drop-deposited onto a 200 mesh Cu grid coated with a holey C-coated support film (SPI supplies). Microscopy images were obtained with a dedicated scanning transmission electron microscope (STEM, 2700Cs, Hitachi) operated at an acceleration voltage of 200 kV. A secondary electron (SE) or high angular annular dark field (HAADF) detector was used for image acquisition.

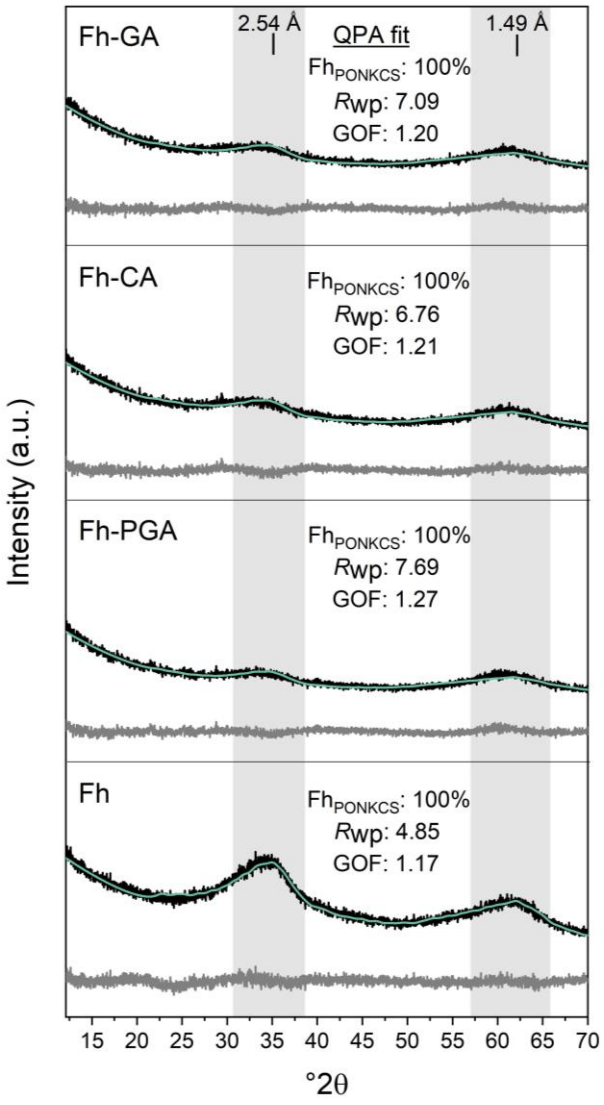

Figure S2. X-ray diffraction patterns and quantitative phase analysis (QPA) of unreacted (co)precipitates including the PONCKS phase. The low goodness of fit (GOF) parameter (<1.3) for each XRD pattern indicates that all samples are well represented by the PONKCS phase during QPA. Light gray bars indicate ferrihydrite features. Figure was originally published in ref. 3.

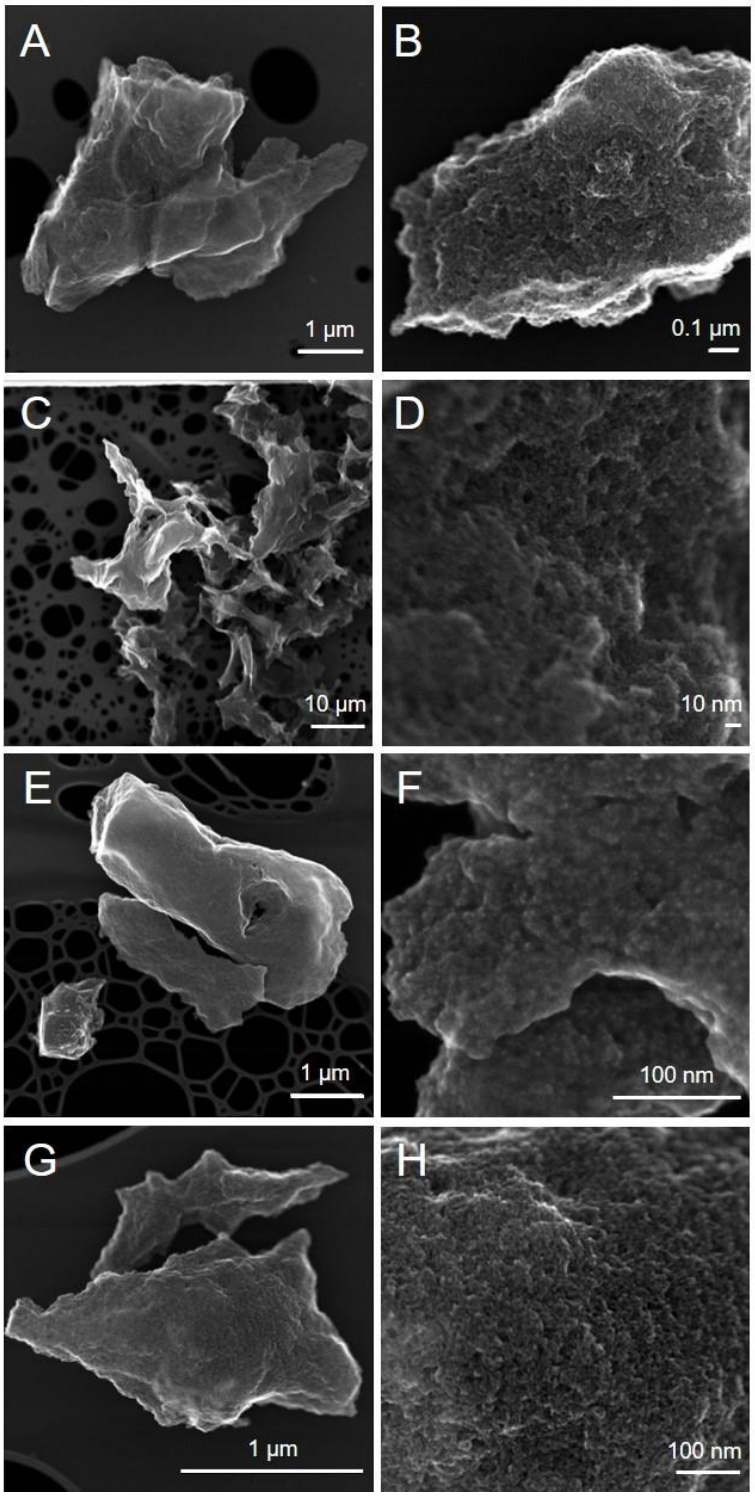

Figure S3. Secondary electron (SE) images of unreacted (co)precipitates. (A,B) Fh. (C,D) Fh-PGA. (E,F) Fh-CA. (G,H) Fh-GA. All (co)precipitates are densely aggregated, likely an effect of flash-freezing and freeze-drying. Figure was originally published in ref. 3.

3. Experimental conditions

Table S2. Elemental composition of unreacted (co)precipitates and S(-II) reacted samples after 1 week.[a]

Sample	Unreacted[b]			Reacted with[c] 1 mM S(-II), 1 wk				Reacted with[c] 5 mM S(-II), 1 wk				Reacted with[c] 1 mM S(-II), 12 mo				Reacted with[c] 5 mM S(-II), 12 mo			
	C	Fe	C/Fe molar ratio	C	Fe	S	C/Fe molar ratio	C	Fe	S	C/Fe molar ratio	C	Fe	S	C/Fe molar ratio	C	Fe	S	C/Fe molar ratio
	(mg/g)		(mol/mol)	(mg/g)		(mg/kg)	(mol/mol)	(mg/g)		(mg/kg)	(mol/mol)	(mg/g)		(mg/kg)	(mol/mol)	(mg/g)		(mg/kg)	(mol/mol)
Fh	1	552	-[d]	8	584	29	0.06	7	396	114	0.08	7	591	22	0.06	14	503	127	0.13
Fh-PGA	62	483	0.60	6	483	17	0.62	67	384	103	0.81	63	570	16	0.51	67	513	102	0.61
Fh-CA	53	471	0.52	5	459	27	0.60	59	458	117	0.60	49	551	13	0.41	39	491	145	0.37
Fh-GA	61	524	0.54	5	482	25	0.53	53	506	129	0.49	44	486	19	0.42	51	562	109	0.42

[a]Determined in at least duplicates. [b]Determined via CHNS (C, S) and ICP-OES (Fe) after being dissolved in concentrated HCl. [c]Determined on 0.45-µm filter residues collected after one week or 12 months with CHNS (C, S). For total Fe contents, samples were dissolved in concentrated HCl and measured with AAS. [d]Value is <0.01.

Table S3. Experimental conditions for the addition of 1 and 5 mM S(-II).

Sample	SSA[a]	PZC[b]	C/Fe molar ratio	Solid:[c] solution ratio	+ 1 mM S(-II)			+ 5 mM S(-II)		
					S(-II)/Fh	S(-II)/Fe(III)	S(-II)/C	S(-II)/Fh	S(-II)/Fe(III)	S(-II)/C
	(m^2/g)	(-)	(mol/mol)	(g/L)	(mmol/g)	(mol/mol)		(mmol/g)	(mol/mol)	
Fh	296	8.2	-[d]	1.01	0.99	0.1	-	4.94	0.5	-
Fh-PGA	155	<3	0.60	1.16	0.99	0.1	0.17	4.94	0.5	0.85
Fh-CA	2.9	4.1	0.52	1.19	0.99	0.1	0.18	4.94	0.5	0.93
Fh-GA	212	5.4	0.54	1.07	0.99	0.1	0.19	4.94	0.5	0.96

[a]Specific surface area estimated via 11-point N_2-BET analysis and corrected for N_2 adsorption onto the OM.[3-5] [b]Determined with electrophoretic mobility measurements as described in ref. 3.[c]To achieve 10 mmol Fe(III)/L. [d]Value is <0.01.

4. Principle component analysis and Target-transform testing

In order to evaluate suitable references for linear combination fitting (LCF) of Fe K-edge EXAFS spectra of sulfide-reacted samples (n = 16), we employed principal component analysis and target-transform testing (PCA-TT) using SixPack.[6] The results of the PCA analysis performed on k^3-weighted EXAFS spectra over 2-12 Å^{-1} are shown in Table S4. Based on the IND function, PCA of Fe K-edge EXAFS spectra indicated eleven statistically significant spectral components, accounting for 99.9% of spectral variance. However, a fit comprising 8 components also described 99.9% of the spectral variance (Table S4), and EXAFS features were not visible in components 9-16. Because all sample spectra were suitabely fit with a set of eight components (selected sample reconstructions based on the first eight components are shown in Figure S4), target-transform testing (TT) and LCF fits were conducted with at most eight fit references.

The relevance of specific reference spectra for LCF was determined by target-transform testing of k^3-weighted Fe (k-range = 2-12 Å^{-1}) spectra. The E_0 of all spectra and reference compounds was set to 7128 eV (Fe). The quality of the transformation was evaluated by the empirical SPOIL value:[7] 0-1.5 excellent, 1.5-3 good, 3-4.5 fair, 4.5-6 acceptable, and >6 for an unacceptable reference spectrum. All Fe references tested had low SPOIL values (<6), and were thus considered in LCF analyses.

Table S4. PCA output parameters for Fe.

Component	Eigenvalue	Cum. Variance	IND
1	67.372	0.881	0.00609
2	4.623	0.941	0.00357
3	2.319	0.972	0.002
4	1.074	0.986	0.00115
5	0.433	0.992	0.00094
6	0.349	0.996	0.00048
7	0.134	0.998	0.00029
8	0.052	0.999	0.00026
9	0.044	0.999	0.00012
10	0.013	0.999	0.000085
11	0.005	0.999	0.0000806
12	0.003	0.999	0.000093
13	0.002	0.999	0.0001
14	0.001	0.999	0.00012
15	0	0.999	0.00041
16	0	1	NA

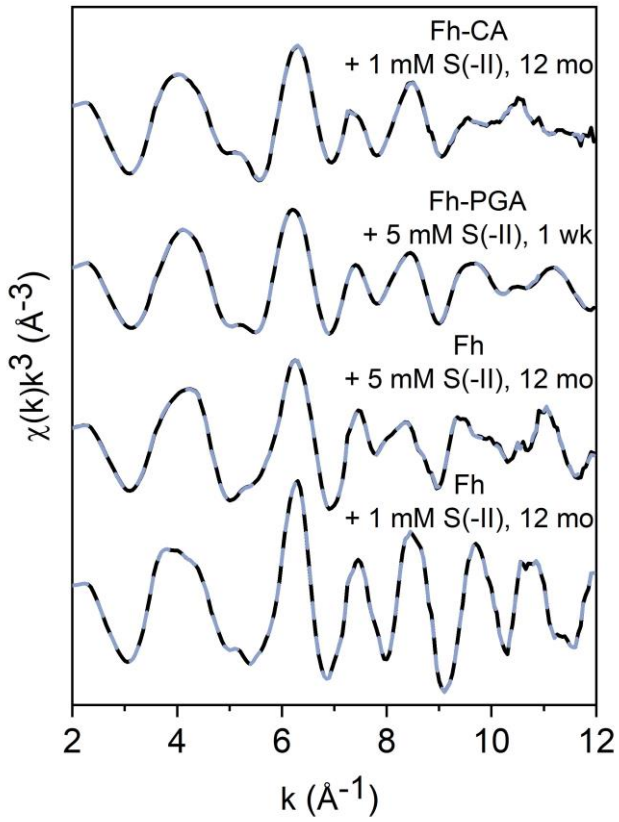

Figure S4. (A) Reconstructions of Fe K-edge EXAFS spectra of selected samples by the first eight PCA components. Experimental data is shown in black, while the spectral reconstructions are shown in blue.

Table S5. Results from Fe target-transform testing.

Reference	Source/ synthesis ref.	χ^2	NSSR[a] (%)	SPOIL
Fe(II)-D-gluconate dihydrate[b]	commercial (Aldrich)	438	0.48	1.38
Fe(III)-citrate[b]	commercial (Fluka)	229	0.14	1.13
Ferrihydrite	synthetic[8]	23	0.02	2.56
Goethite	synthetic[9]	59	0.03	1.47
Green rust (chloride)[c]	Courtesy of T. Borch	260	0.25	0
Lepidocrocite[b]	synthetic[10]	61	0.02	0.1
Mackinawite[d]	Courtesy of E. D. Burton	117	0.08	2.15
Magnetite[b,e]	natural	339	0.13	0.63
Pyrite[b,e]	natural	363	0.05	0

[a]Normalized sum of squared residuals ($100\times\sum_i(data_i\text{-}fit_i)^2/\sum_i data_i^2$). [b]Spectrum from ref. [11]. [c]Spectrum courtesy of T. Borch (Colorado State University, USA). [d]Spectrum courtesy of E. D. Burton (Southern Cross University, Australia). [e]Sample provided by the ETH Zurich, Switzerland.

5. Aqueous S and Fe concentrations and speciation.

Table S6. PCA output parameters for Fe.

HPLC	**Agilent 1290 Quaternary**
Column	Hamilton PRP-X100, 125 x 40 mm, 10 µm
Injection volume	50 µL
Mobile phase	Ammonium carbonate 100 mM, pH 9.5
Flow rate	1.5 mL min^{-1}
ICP-MS	**Agilent 8800 ICP-QQQ**
Configuration	Pt cones and x-lenses
Spray chamber	Scott double pass, +2 °C
RF power	1500 W
Nebulizer	Glass, microcentric
Nebulizer gas	0.99 L min^{-1}
Makeup gas	0.1 L min^{-1}
Optional gas (20% O_2 in Ar)	5%
Cell gas	30% O_2 in 1 mL min^{-1} of H_2
Monitored masses	S:32 to 46 and 34 to 50; Sc: 45 to 61; Y: 89 to 105
Acquisition time	50 ms for S and 30 ms for Sc and Y

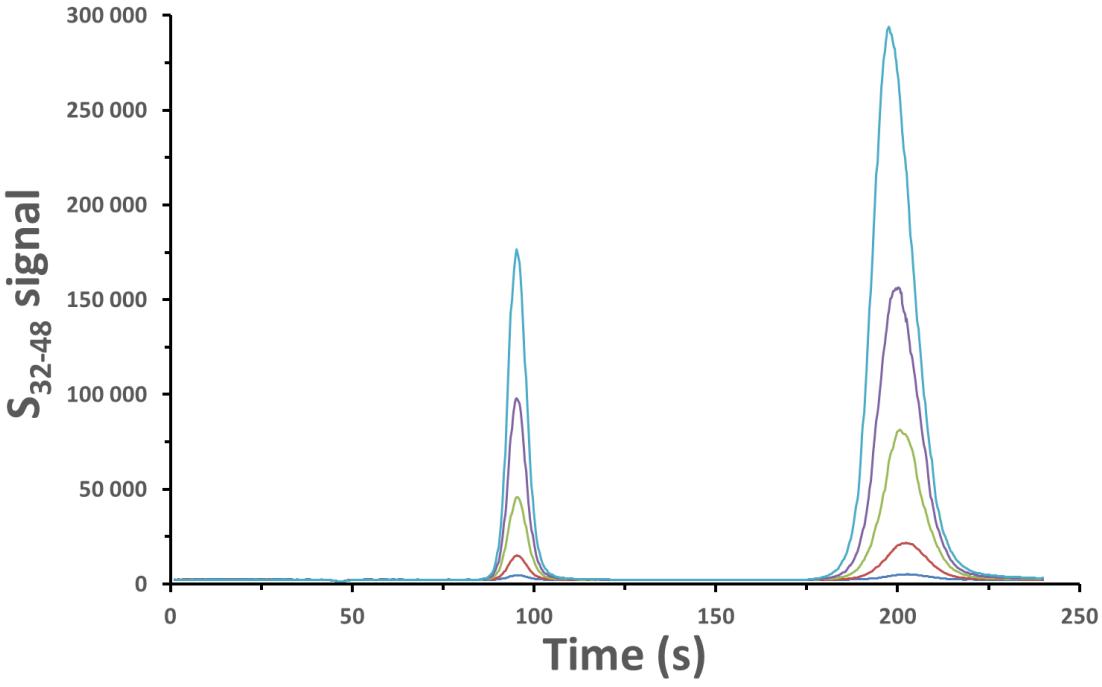

Figure S5: Typical chromatograms for standards of sulfate (2, 10, 25, 50 and 100 µmol L^{-1}) and thiosulfate (5, 20, 50, 100 and 200 µmol L^{-1}) when analyzed by HPLC-ICP-MS/MS.

Table S7. Aqueous sulfate and thiosulfate concentrations.

Sample		Time	Sulfate	Thiosulfate	S_2O_3/SO_4
		(hours)	(µM)		(-)
+ 1 mM S(-II)	**Fh**	6	NM[a]	NM[a]	
		24	5.1 (0.4)	29.7 (4.4)	5.8
		48	5.7 (0.6)	32.2 (2.8)	5.6
		168	7.6 (0.5)	45.8 (2.6)	6.1
		12 months[b]	9.3 (0.4)	59.8 (5.1)	6.5
	Fh-PGA	6	NM[a]	NM[a]	
		24	6.9 (1.6)	43.8 (3.6)	6.4
		48	6.8 (0.5)	42.9 (2.2)	6.3
		168	6.0 (0.4)	42.3 (2.5)	7.1
		12 months[b]	9.8 (1.3)	67.4 (2.5)	6.9
	Fh-CA	6	NM[a]	NM[a]	
		24	7.4 (1.7)	49.2 (5.1)	6.7
		48	7.2 (0.2)	47.1 (0.5)	6.5
		168	7.6 (1.3)	40.1 (3.2)	5.3
		12 months[b]	10.1 (1.0)	59.1 (2.1)	5.9
	Fh-GA	6	NM[a]	NM[a]	
		24	8.9 (1.2)	51.3 (2.6)	5.8
		48	10.4 (0.8)	48.4 (0.9)	4.7
		168	8.8 (0.2)	44.4 (5.0)	5.1
		12 months[b]	8.8 (6.9)	61.1 (2.4)	6.9
+ 5 mM S(-II)	**Fh**	6	24.8 (0.5)	174.9 (3.5)	7.0
		24	24.3 (1.2)	164.9 (1.5)	6.8
		48	26.2 (3.6)	170.1 (5.1)	6.5
		168	22.9 (0.9)	161.8 (0.3)	7.1
		12 months[b]	28.6 (0.4)	178.1 (6.6)	6.2
	Fh-PGA	6	25.5 (1.2)	160.5 (2.7)	6.3
		24	28.1 (0.7)	165.5 (4.7)	5.9
		48	25.0 (1.0)	159.1 (12.8)	6.4
		168	25.0 (1.9)	174.5 (1.2)	7.0
		12 months[b]	30.6 (8.1)	200.1 (1.5)	6.5
	Fh-CA	6	29.3 (2.5)	166.7 (22.4)	5.7
		24	26.0 (1.3)	148.0 (8.7)	5.7
		48	26.2 (1.2)	146.6 (5.1)	5.6
		168	26.0 (1.0)	147.7 (4.7)	5.7
		12 months[b]	35.1 (4.0)	188.1 (6.1)	5.4
	Fh-GA	6	30.0 (2.1)	152.6 (6.4)	5.1
		24	28.1 (1.5)	154.5 (10.8)	5.5
		48	28.7 (0.3)	153.7 (7.6)	5.4
		168	29.6 (1.3)	153.8 (7.1)	5.2
		12 months[b]	37.0 (1.2)	229.0 (12.0)	6.2

Parameter uncertainties are given in parentheses for the last significant figure. [a]Concentrations were not determined. [b]Please note the that this timepoint refers to months.

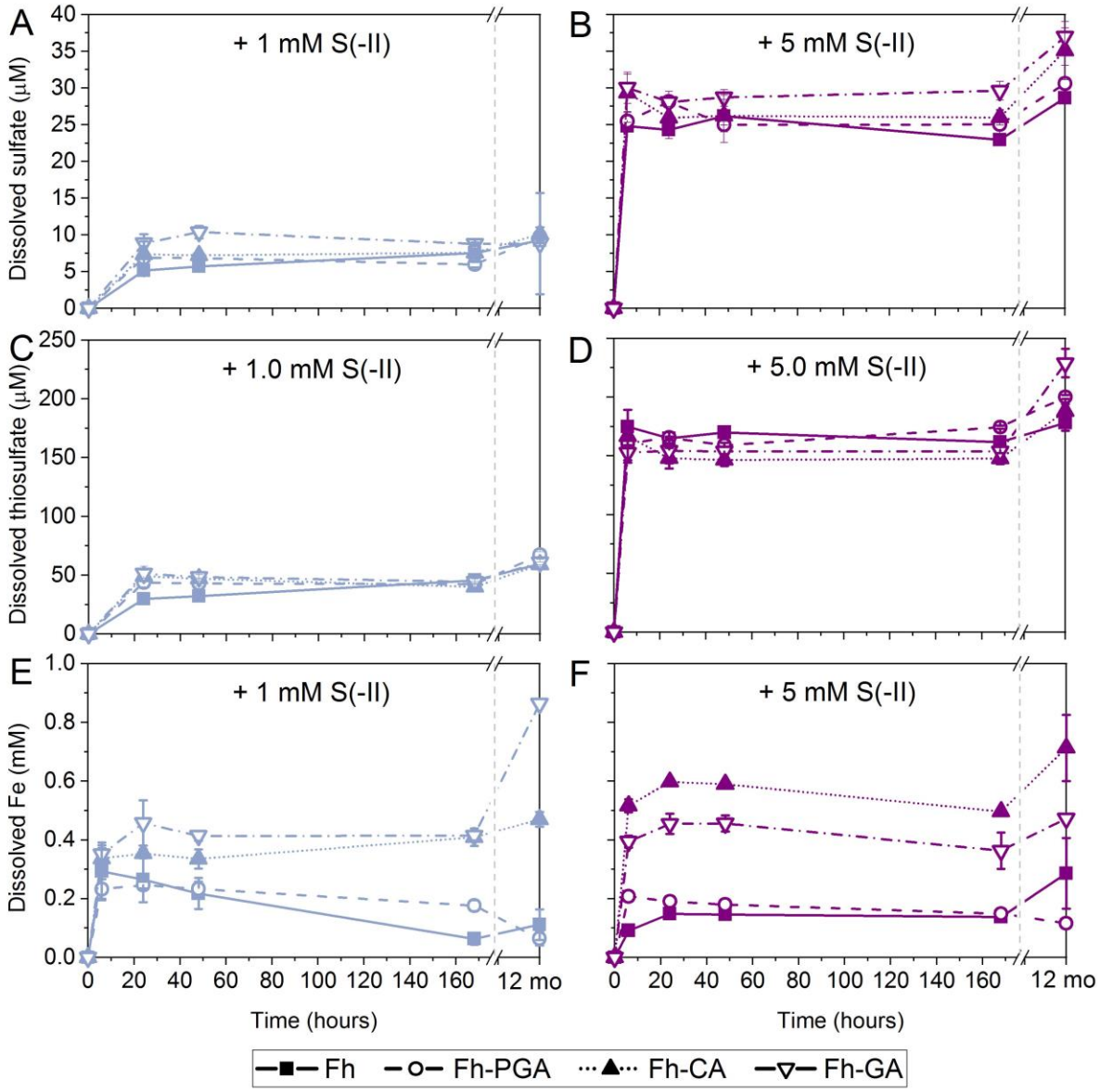

Figure S6. Trends in dissolved sulfate, thiosulfate, and Fe (Fe_{aq}) for samples reacted with (A) 1 or (B) 5 mM S(-II). Please note the break in the x-axis. Dissolved Fe concentrations in the sulfide-free controls, measured at 1 week (168 hrs) and 12 months, was negligible (≤0.02 mM).

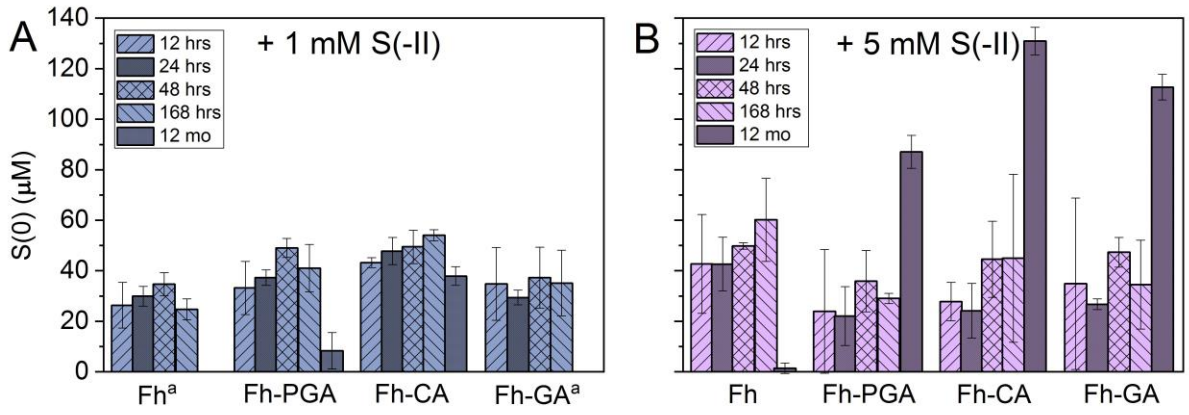

Figure S7. Elemental S (S(0)) determined in chloroform extractions of unfiltered samples during reaction with (A) 1 mM S(-II) and (B) 5 mM S(-II). Concentrations in 0.22-µm filtered samples were negligible (data not shown). Error bars indicate the standard deviation calculated from triplicate experiments. [a]S(0) was below detection limits for Fh and Fh-GA reacted with 1 mM S(-II) at 12 months.

6. Solid-phase Fe speciation: XAS

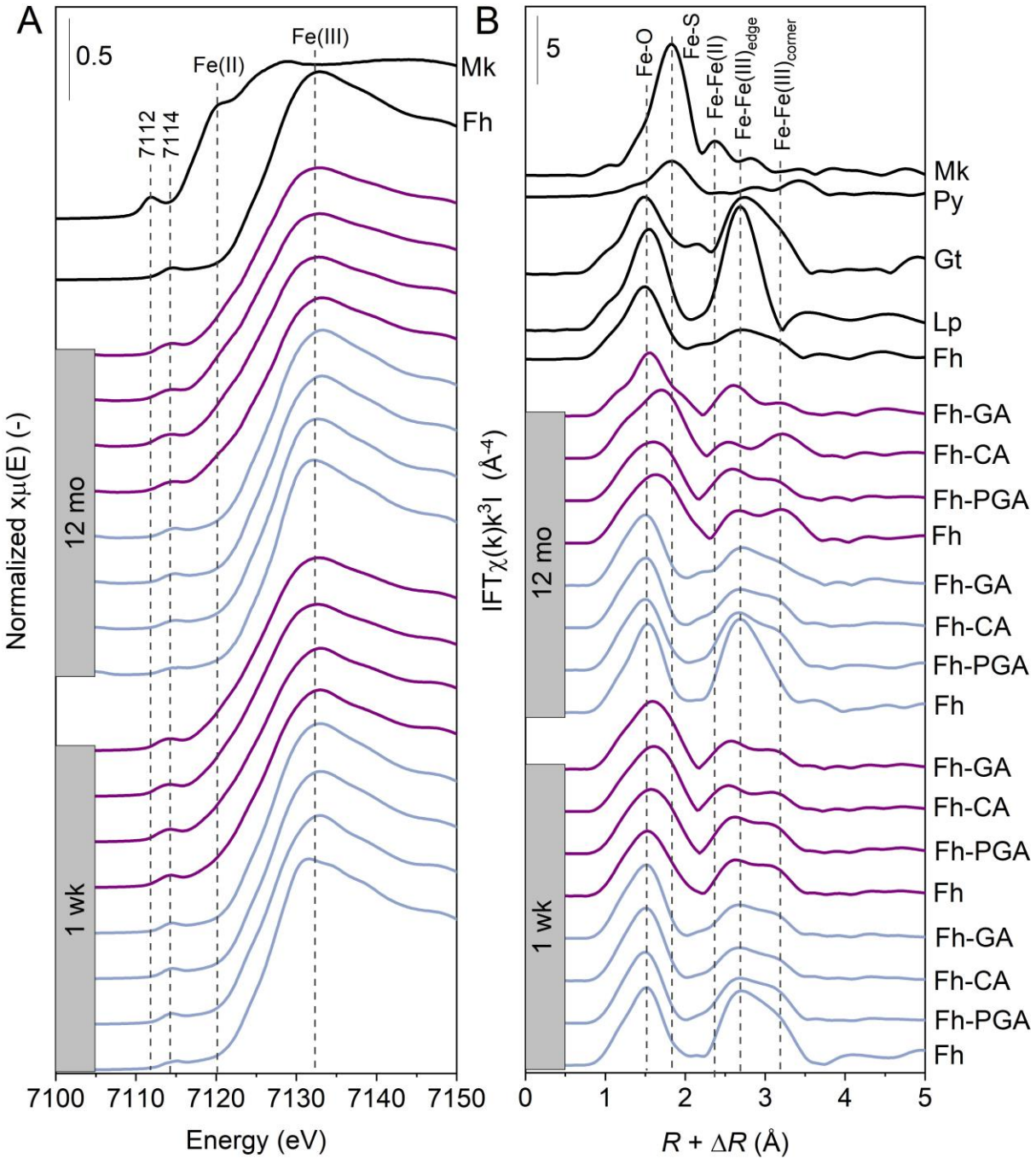

Figure S8. (A) Normalized Fe K-edge XANES spectra of (co)precipitates reacted with 1 and 5 mM S(-II) (shown in Blue and Purple, respectively) for one week (1 wk) and 12 months (12 mo), and Fe(II/III) reference compounds. (B) Fourier-transform magnitudes of the corresponding Fe EXAFS spectra. Abbreviations: Fh = ferrihydrite, Gt = goethite, Lp = lepidocrocite, Mk = mackinawite, Py = pyrite.

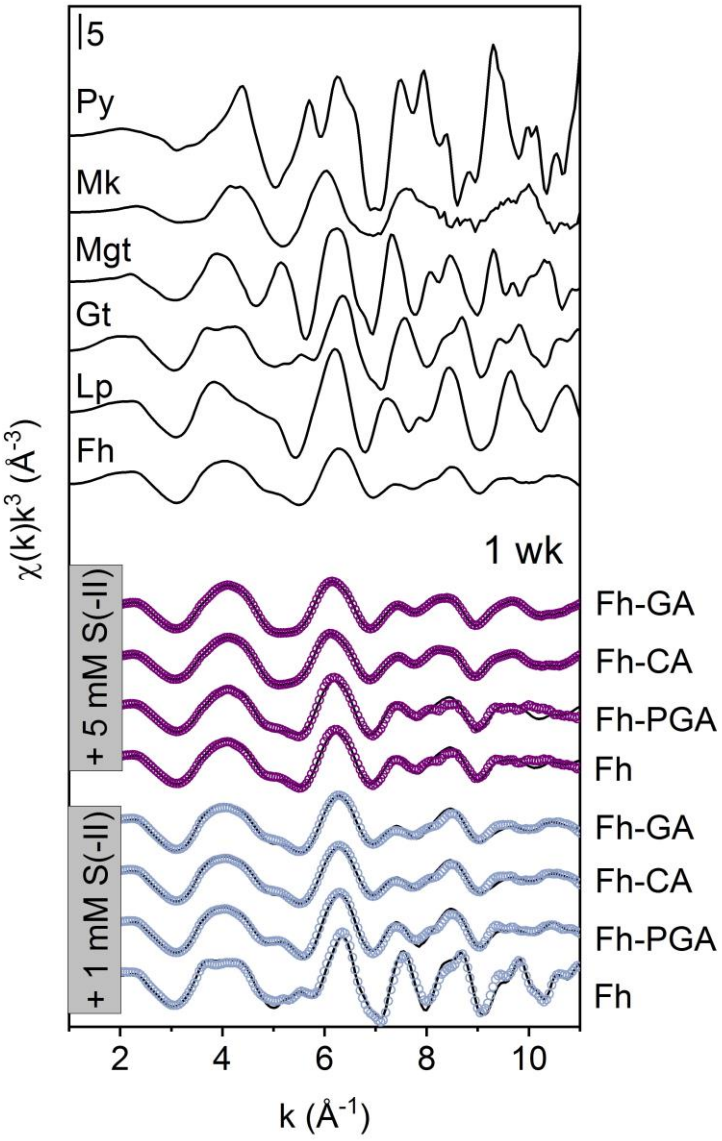

Figure S9. Iron K-edge EXAFS spectra of 1 week S(-II)-reacted (co)precipitates and reference spectra. Experimental data and model fits are shown as solid and dotted lines, respectively. Fit parameters are detailed in Table 1 and fit fractions are illustrated in Figure 2B. Abbreviations: Fh = ferrihydrite, Gt = goethite, Lp = lepidocrocite, Mgt = magnetite, Mk = mackinawite, Py = pyrite.

8. Solid-phase S speciation: S XANES

Data processing and deconvolution of the normalized S K-edge XANES spectra was performed using WinXAS 3.0[12] following a modified version of the fitting approaches of Manceau and Nagy[13] and Shakeri Yetka et al.[14] over an energy range of 2466-2488 eV. Briefly, deconvolution of S(-II)-reacted samples included a set of four Gaussians for the S s → p transition peaks and an arctangent function at ~2475. Because all 'reduced' S species show a strong post-edge adsorption feature in the range 2475-2482 eV[15] and fitting of Gaussian curves in this energy range in S XANES samples dominated by 'reduced' S species can lead to misinterpretation of 'oxidized' S species fractions,[13] one additional Gaussian, positioned at ca. 2478 eV with a broad FWHM, was fit in all samples and, combined with the arctan, represented the post-edge absorption of 'reduced' S species. In all samples, a distinct feature, separate from the 'reduced' S species post-edge adsorption, was visible at ~2481 eV and thus fit with one of the Gaussians as sulfonate. Positions and heights of all Gaussians were varied in all fits, while the full width at half maximum of the dominant 'reduced' S species were correlated. The areas of the Gaussians were calculated and subsequently corrected for the oxidation state-dependent change in the absorption cross-section based on the generic curve described in Manceau and Nagy.[13] To calculate the relative contribution of every S species to the total S in the sample, the corrected peak area for each S species was normalized to the peak-area sum of all identified S species.

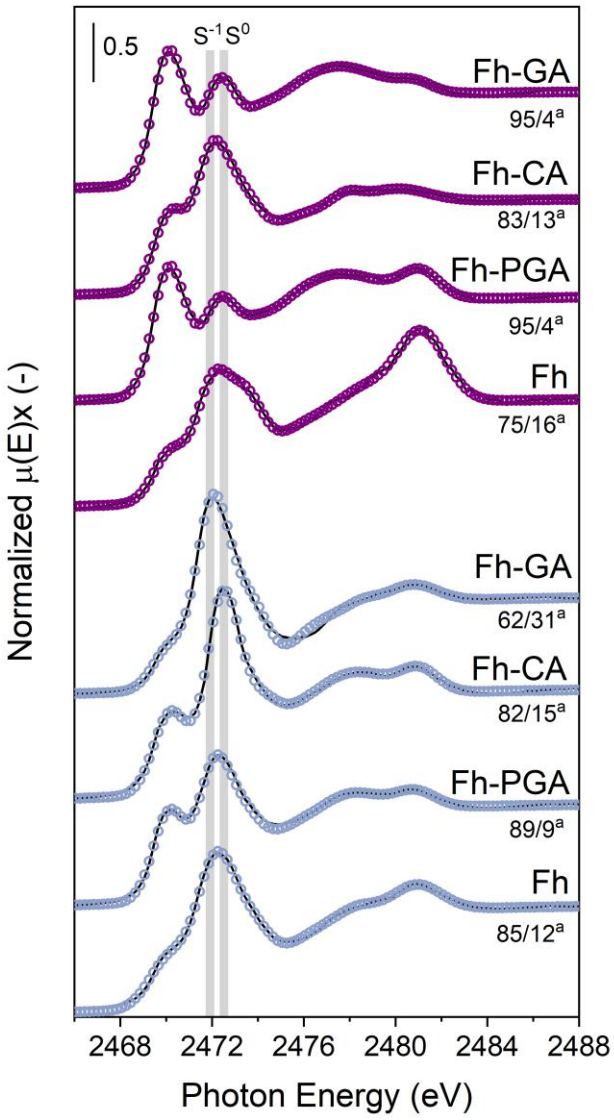

Figure S10. Normalized S K-edge XANES spectra and deconvolution fits for samples reacted with 1 or 5 mM S(-II) for 12 months, shown in blue and purple, respectively. The spectra were decomposed into 4 Gaussians and 1 arctangent functions. The broad peak feature at ~2475−2479 eV is a postedge absorption feature of the reduced S species[13,15] and thus was included in the background. [a]Contributions from [Inorganic sulfide]/[Org. Exocyclic/Elemental S]. Fit parameters are detailed in Table S8.

Table S8. Gaussian deconvolution of normalized S K-edge XANES spectra.

Sample	Arctan + S Species	Energy[a] (eV)	FWHM[b]	Height	Area	SF[c]	Corrected Area	Fraction (%)	NSSR[d] (%)
Fh + 1 mM S(-II) 1 wk	Arctan	2475.23	2.17	1.01					1.6
	Inorganic Sulfide	2470.07	1.75	0.69	1.28	0.03	45.00	89.6	
	Exocyclic/ elemental	2472.48	1.75	2.07	3.86	0.92	4.22	8.4	
	Heterocyclic	2474.27	1.75	0.69	1.28	1.58	0.81	1.6	
	Sulfonate	2480.93	2.25	0.30	0.72	4.03	0.18	0.4	
Fh + 5 mM S(-II) 1 wk	Arctan	2474.02	3.35	1.03					1.1
	Inorganic Sulfide	2470.15	1.70	0.96	1.74	0.06	30.73	89.1	
	Exocyclic/ elemental	2472.40	1.70	1.56	2.82	0.89	3.17	9.2	
	Heterocyclic	2473.87	1.70	0.42	0.76	1.43	0.53	1.5	
	Sulfonate	2481.00	1.83	0.14	0.28	4.06	0.07	0.2	
Fh + 1 mM S(-II) 12 mo	Arctan	2475.14	4.00	1.07					1.4
	Inorganic Sulfide	2470.10	2.00	0.44	0.94	0.04	25.04	84.9	
	Exocyclic/ elemental	2472.16	2.00	1.31	2.78	0.80	3.48	11.8	
	Heterocyclic	2473.81	2.00	0.54	1.14	1.41	0.81	2.8	
	Sulfonate	2480.93	2.51	0.25	0.66	4.03	0.16	0.6	
Fh + 5 mM S(-II) 12 mo	Arctan	2474.54	3.99	1.09					1.4
	Inorganic Sulfide	2470.18	1.73	0.45	0.84	0.07	11.93	75.1	
	Exocyclic/ elemental	2472.05	1.73	1.03	1.90	0.76	2.50	15.7	
	Heterocyclic	2473.52	1.73	0.72	1.33	1.30	1.02	6.4	
	Sulfonate	2481.11	2.50	0.68	1.80	4.09	0.44	2.8	
Fh-PGA + 1 mM S(-II) 1 wk	Arctan	2475.29	2.35	1.02					1.5
	Inorganic Sulfide	2470.19	1.74	0.57	1.05	0.07	14.42	72.6	
	Exocyclic/ elemental	2472.49	1.74	2.18	4.03	0.92	4.39	22.1	
	Heterocyclic	2474.22	1.74	0.68	1.25	1.56	0.80	4.0	
	Sulfonate	2480.98	2.07	0.48	1.06	4.05	0.26	1.3	
Fh-PGA + 5 mM S(-II) 1 wk	Arctan	2474.00	3.61	0.98					1.1
	Inorganic Sulfide	2470.15	1.71	1.25	2.27	0.06	39.16	94.4	
	Exocyclic/ elemental	2472.34	1.71	0.94	1.71	0.86	1.98	4.8	
	Heterocyclic	2473.77	1.71	0.25	0.46	1.39	0.33	0.8	
	Sulfonate	2480.80	1.89	0.05	0.11	3.98	0.03	0.1	

[a]Energy of the white-line maximum. [b]Full width at half maximum. Parameters with identical numbers were correlated during fitting. [c]Scaling factor based on the 'generic' equation of Manceau and Nagy.[13] [d]Normalized sum of squared residuals ($100\times\sum_i(data_i\text{-}fit_i)^2/\sum_i data^2$).

Table S8. *Continued.*

Fh-PGA + 1 mM S(-II) 12 mo	Arctan	2474.00	4.00	1.02					1.4
	Inorganic Sulfide	2470.14	1.66	0.82	1.45	0.05	26.79	88.9	
	Exocyclic/ elemental	2472.11	1.66	1.15	2.04	0.78	2.61	8.7	
	Heterocyclic	2473.41	1.66	0.47	0.82	1.26	0.65	2.2	
	Sulfonate	2480.84	2.07	0.16	0.35	3.99	0.09	0.3	
Fh-PGA + 5 mM S(-II) 12 mo	Arctan	2474.00	3.71	1.04					1.3
	Inorganic Sulfide	2470.16	1.68	1.21	2.15	0.06	35.57	94.6	
	Exocyclic/ elemental	2472.28	1.68	0.74	1.32	0.84	1.57	4.2	
	Heterocyclic	2473.60	1.68	0.25	0.44	1.33	0.33	0.9	
	Sulfonate	2481.10	1.92	0.24	0.48	4.09	0.12	0.3	
Fh-CA + 1 mM S(-II) 1 wk	Arctan	2474.93	3.54	1.03					1.3
	Inorganic Sulfide	2470.21	1.67	0.61	1.08	0.08	13.84	71.9	
	Exocyclic/ elemental	2472.47	1.67	2.30	4.09	0.91	4.48	23.2	
	Heterocyclic	2474.03	1.67	0.66	1.18	1.49	0.79	4.1	
	Sulfonate	2480.94	2.06	0.28	0.61	4.03	0.15	0.8	
Fh-CA + 5 mM S(-II) 1 wk	Arctan	2474.00	3.64	0.99					1.2
	Inorganic Sulfide	2470.15	1.66	1.10	1.94	0.06	33.41	91.6	
	Exocyclic/ elemental	2472.39	1.66	1.27	2.24	0.88	2.54	7.0	
	Heterocyclic	2473.83	1.66	0.39	0.69	1.41	0.49	1.3	
	Sulfonate	2480.75	1.72	0.06	0.11	3.96	0.03	0.1	
Fh-CA + 1 mM S(-II) 12 mo	Arctan	2474.09	4.00	1.11					1.4
	Inorganic Sulfide	2470.19	1.73	0.75	1.38	0.07	18.94	81.9	
	Exocyclic/ elemental	2472.47	1.73	1.72	3.17	0.91	3.47	15.0	
	Heterocyclic	2474.01	1.73	0.39	0.71	1.48	0.48	2.1	
	Sulfonate	2481.04	1.91	0.21	0.91	4.07	0.22	1.0	
Fh-CA + 5 mM S(-II) 12 mo	Arctan	2474.00	3.54	0.96					1.1
	Inorganic Sulfide	2470.18	1.66	0.71	1.25	0.07	18.44	83.0	
	Exocyclic/ elemental	2472.02	1.66	1.21	2.13	0.75	2.86	12.9	
	Heterocyclic	2473.36	1.66	0.57	1.00	1.24	0.81	3.6	
	Sulfonate	2480.03	3.23	0.13	0.46	3.70	0.12	0.6	

[a]Energy of the white-line maximum. [b]Full width at half maximum. Parameters with identical numbers were correlated during fitting. [c]Scaling factor based on the 'generic' equation of Manceau and Nagy.[13] [d]Normalized sum of squared residuals ($100\times\sum_i(data_i\text{-}fit_i)^2/\sum_i data^2$).

Table S8. *Continued.*

Fh-GA + 1 mM S(-II) 1 wk	Arctan	2475.02	2.66	1.04					1.5
	Inorganic Sulfide	2470.19	1.66	0.66	1.16	0.07	16.36	75.4	
	Exocyclic/ elemental	2472.51	1.66	2.24	3.96	0.93	4.27	19.7	
	Heterocyclic	2474.13	1.66	0.71	1.25	1.52	0.82	3.8	
	Sulfonate	2480.99	2.16	0.42	0.96	4.05	0.24	1.1	
Fh-GA + 5 mM S(-II) 1 wk	Arctan	2474.00	3.55	0.99					1.2
	Inorganic Sulfide	2470.13	1.67	1.24	2.20	0.05	42.32	94.9	
	Exocyclic/ elemental	2472.35	1.67	0.90	1.60	0.87	1.84	4.1	
	Heterocyclic	2473.82	1.67	0.26	0.46	1.41	0.32	0.7	
	Sulfonate	2480.97	1.62	0.25	0.42	4.04	0.10	0.2	
Fh-GA + 1 mM S(-II) 12 mo	Arctan	2475.48	4.00	0.97					2.0
	Inorganic Sulfide	2470.15	1.75	0.38	0.71	0.06	12.66	70.7	
	Exocyclic/ elemental	2472.06	1.75	1.74	3.22	0.76	4.24	23.7	
	Heterocyclic	2473.70	1.75	0.65	1.21	1.37	0.89	5.0	
	Sulfonate	2480.72	2.51	0.17	0.45	3.95	0.11	0.6	
Fh-GA + 5 mM S(-II) 12 mo	Arctan	2474.00	3.67	0.97					1.5
	Inorganic Sulfide	2470.15	1.67	1.24	2.22	0.06	38.47	95.0	
	Exocyclic/ elemental	2472.32	1.67	0.84	1.49	0.86	1.74	4.3	
	Heterocyclic	2473.78	1.67	0.21	0.37	1.40	0.26	0.6	
	Sulfonate	2480.88	1.66	0.08	0.14	4.01	0.04	0.1	

[a]Energy of the white-line maximum. [b]Full width at half maximum. Parameters with identical numbers were correlated during fitting. [c]Scaling factor based on the 'generic' equation of Manceau and Nagy.[13] [d]Normalized sum of squared residuals ($100\times\sum_i(data_i\text{-}fit_i)^2/\sum_i data^2$).

Table S9. Ratios of 'reduced' S species formed.[a]

Sample		Inorganic Sulfide: Exocyclic/elemental	Inorganic Sulfide: Heterocyclic	Exocyclic/elemental: Heterocyclic
+ 1 mM S(-II) 1 wk	Fh	10.7	55.5	5.2
	Fh-PGA	3.3	17.9	5.5
	Fh-CA	3.1	17.5	5.7
	Fh-GA	3.8	19.9	5.2
+ 5 mM S(-II) 1 wk	Fh	9.7	58.2	6.0
	Fh-PGA	19.7	118.7	6.0
	Fh-CA	13.1	68.4	5.2
	Fh-GA	23.0	130.6	5.7
+ 1 mM S(-II) 12 mo	Fh	7.2	30.8	4.3
	Fh-PGA	10.3	41.0	4.0
	Fh-CA	5.5	39.2	7.2
	Fh-GA	3.0	14.3	4.8
+ 5 mM S(-II) 12 mo	Fh	4.8	11.7	2.4
	Fh-PGA	22.6	107.8	4.8
	Fh-CA	6.4	22.9	3.6
	Fh-GA	22.1	146.6	6.6

[a]Calculated from Table S8.

9. References

1. Schwertmann, U.; Cornell, R. M., *Iron Oxides in the Laboratory: Preparation and Characterization*. WILEY-VCH Verlag GMBH & Co. KGaA: Weinheim, Germany, 2000.
2. Hofmann, A.; Pelletier, M.; Michot, L.; Stradner, A.; Schurtenberger, P.; Kretzschmar, R., Characterization of the pores in hydrous ferric oxide aggregates formed by freezing and thawing. *J. Colloid Interf. Sci.* **2004,** *271*, 163-173.
3. ThomasArrigo, L. K.; Kaegi, R.; Kretzschmar, R., Ferrihydrite growth and transformation in the presence of ferrous Fe and model organic ligands. *Environ. Sci. Technol.* **2019,** *53*, 13636-13647.
4. Mikutta, C.; Mikutta, R.; Bonneville, S.; Wagner, F.; Voegelin, A.; Christl, I.; Kretzschmar, R., Synthetic coprecipitates of exopolysaccharides and ferrihydrite. Part 1: Characterization. *Geochim. Cosmochim. Acta* **2008,** *72*, 1111-1127.
5. Mikutta, R.; Mikutta, C., Stabilization of organic matter at micropores (<2 nm) in acid forest subsoils. *Soil Sci. Soc. Am. J.* **2006,** *70*, 2049-2056.
6. Webb, S. M., SIXPack: A graphical user interface for XAS analysis using IFEFFIT. *Phys. Scripta* **2005,** *T115*, 1011-1014.
7. Malinowski, E. R., Theory of error for target factor-analysis with applications to mass-spectrometry and nucelar magnetic-resonance spectrometry. *Anal. Chim. Acta* **1978,** *2*, 339-354.
8. ThomasArrigo, L. K.; Mikutta, C.; Byrne, J.; Kappler, A.; Kretzschmar, R., Iron(II)-catalyzed iron atom exchange and mineralogical changes in iron-rich organic freshwater flocs: An iron isotope tracer study. *Environ. Sci. Technol.* **2017,** *51*, 6897-6907.

9. Mikutta, C.; Wiederhold, J. G.; Cirpka, O. A.; Hofstetter, T. B.; Bourdon, B.; Von Gunten, U., Iron isotope fractionation and atom exchange during sorption of ferrous iron to mineral surfaces. *Geochim. Cosmochim. Acta* **2009,** *73*, 1795-1812.
10. Borer, P.; Sulzberger, B.; Hug, S. J.; Kraemer, S. M.; Kretzschmar, R., Photoreductive dissolution of iron(III) (hydr)oxides in the absence and presence of organic ligands: Experimental studies and kinetic modeling. *Environ. Sci. Technol.* **2009,** *43*, 1864-1870.
11. Langner, P.; Mikutta, C.; Kretzschmar, R., Arsenic sequestration by organic sulphur in peat. *Nat. Geosci.* **2012,** *5*, 66-73.
12. Ressler, T., WinXAS: A program for X-ray absorption spectroscopy data analysis under MS-Windows. *J. Synchrotron Radiat.* **1998,** *5*, 118-122.
13. Manceau, A.; Nagy, K. L., Quantitative analysis of sulfur functional groups in natural organic matter by XANES spectroscopy. *Geochim. Cosmochim. Acta* **2012,** *99*, 206-223.
14. Shakeri Yekta, S.; Gustavsson, J.; Svensson, B. H.; Skyllberg, U., Sulfur K-edge XANES and acid volatile sulfide analyses of changes in chemical speciation of S and Fe during sequential extraction of trace metals in anoxic sludge from biogas reactors. *Talanta* **2012,** *89*, 470-477.
15. Morgan, B.; Burton, E. D.; Rate, A. W., Iron monosulfide enrichment and the presence of organosulfur in eutrophic estuarine sediments. *Chem. Geol.* **2012,** *296*, 119-130.